



## Subcortical atrophy correlates with the perturbational complexity index in patients with disorders of consciousness

Evan S. Lutkenhoff <sup>a, b</sup>, Micah A. Johnson <sup>a</sup>, Silvia Casarotto <sup>c</sup>, Marcello Massimini <sup>c, d</sup>, Martin M. Monti <sup>a, b, \*</sup>

<sup>a</sup> Department of Psychology, University of California Los Angeles, Los Angeles, CA, USA

<sup>b</sup> Brain Injury Research Center (BIRC), Department of Neurosurgery, David Geffen School of Medicine at UCLA, Los Angeles, CA, USA

<sup>c</sup> Department of Biomedical and Clinical Sciences "L. Sacco", University of Milan, Milan, Italy

<sup>d</sup> IRCCS Fondazione Don Carlo Gnocchi, Milan, Italy

### ARTICLE INFO

#### Article history:

Received 20 September 2019

Received in revised form

26 May 2020

Accepted 21 July 2020

Available online 25 July 2020

#### Keywords:

Consciousness

Disorders of consciousness

Perturbational complexity index

Globus pallidus

### ABSTRACT

**Background:** The complexity of neurophysiological brain responses to direct cortical stimulation, referred to as the perturbational complexity index (PCI), has been shown able to discriminate between consciousness and unconsciousness in patients surviving severe brain injury as well as several other conditions (e.g., wake, dreamless sleep, sleep and ketamine dreaming, anesthesia).

**Objective:** This study asks whether, in patients with a disorder of consciousness (DOC), the complexity of the neurophysiological response to cortical stimulation is preferentially associated with atrophy within specific brain structures.

**Methods:** We perform a retrospective analysis of 40 DOC patients and correlate their maximal PCI to MR-based measurements of cortical thinning and subcortical atrophy.

**Results:** PCI was systematically and inversely associated with the degree of local atrophy within the globus pallidus, a region previously linked to electrocortical and behavioral arousal. Conversely, we fail to detect any association between variance in cortical ribbon thickness and PCI.

**Conclusion:** These findings corroborate the previously reported association between pallidal atrophy and low behavioral arousal and suggest that this region's role in maintaining the overall balance of excitation and inhibition may critically affect the emergence of complex cortical interactions in chronic disorders of consciousness. This finding thus also suggests a target for potential neuromodulatory intervention in DOC patients.

© 2020 The Author(s). Published by Elsevier Inc. This is an open access article under the CC BY-NC-ND license (<http://creativecommons.org/licenses/by-nc-nd/4.0/>).

## Introduction

In the absence of the ability to directly access someone's subjective experience (e.g., via verbal report), assessing someone's capacity of consciousness is an inferential process whereby purposeful, non-reflexive behaviors are typically taken to reveal the presence of consciousness [1,2]. In circumstances where cognitive processing and behavior might be constrained, such as in severely brain-injured patients [3,4], responsiveness to stimulation cannot be relied upon to detect the presence of consciousness [5], giving rise to the risk of misdiagnosis [6–10]. The development of novel

ways to overcome such problem thus has become an imperative in order to mitigate the potentially severe medical, legal, and ethical consequences of misdiagnosis [11,12].

One approach to overcoming the limitations of behavior-based assessments has been the use of so-called "active" neuroimaging paradigms whereby patients engage willfully in a mental task to demonstrate response to command and thus a state of awareness (e.g., mental imagery [13–19]). While showing a remarkable level of specificity in detecting the presence of (minimal) consciousness in patients who appear behaviorally unconscious, and allowing single-patient decision-making, this approach suffers from low sensitivity [14,20], perhaps due to the many ancillary cognitive resources needed, beyond a state of awareness, for a positive response to be detected (e.g., language comprehension, working memory; cf [21]). In parallel, many have focused on "passive" neuroimaging paradigms as a means of detecting patterns of

\* Corresponding author. Department of Psychology, University of California Los Angeles, Los Angeles, CA, 90095, USA.

E-mail address: [monti@ucla.edu](mailto:monti@ucla.edu) (M.M. Monti).

association between specific functional [22–31] and structural [32–35] biomarkers, on the one hand, and state of consciousness and level of cognitive functioning [13,36–42], on the other. These paradigms are appealing because they allow dispensing with assuming sufficient residual integrity of a patient's cognitive abilities. Furthermore, when coupled with machine learning approaches, these methods show the promise of single-patient classification on the basis of structural [43] and functional [44] properties, with decision-hyperplanes often associating a state of consciousness with the presence of large-scale interactions and the complexity of neural dynamics [27,45].

Over the past 10 years, a novel neurophysiological approach has been developed to measure the conjoint existence of large scale interactions (functional integration) and complexity of neural dynamics (functional differentiation) [46–48], based on a combination of transcranial magnetic stimulation and electroencephalography (TMS-EEG). At a high level, this technique can be described with a simple analogy [49]: much like someone might knock on an object and listen to the echo it produces in order to infer its density or internal structure, this technique employs TMS to “knock on the brain” and then listens to the electrocortical response elicited to infer the level of information and integration the system is capable of. As shown previously, the algorithmic complexity of the electrocortical echo elicited as the energy introduced by the TMS pulse dissipates along brain networks (known as the perturbational complexity index, PCI [50]) is systematically related, in a graded fashion [50], to one's state of consciousness [51]. PCI combines the advantages of passive paradigms with the potential for single-subject inference typical of active paradigms (e.g. Ref. [46–48,51]). Similar to passive paradigms, this measure makes no assumptions as to the residual sensory modalities available to a given patient, and does not require them to be able to comprehend and remember instructions, and engage in and disengage from a cognitive task in response to a cue. On the other hand, extensive validation in 540 benchmark measurement sets collected across 150 volunteers during wake, sleep, and different modes of agent-induced loss of consciousness, as well as over 250 measurement sets collected in 81 patients with disorders of consciousness (DOC), allow for single-subject quantitative inference with very high sensitivity (i.e., 94.7% of MCS patients correctly classified [51]) on the basis of a simple and transferrable criterion (i.e.,  $\text{PCI}_{\max} > 0.31$ ). Furthermore, TMS-EEG has also been shown to stratify behaviorally unresponsive patients into subsets characterized by different outcome [51] and specific pathophysiological mechanisms [52], further highlighting the clinical potential of this approach.

From a neurophysiological perspective, the PCI measurement is believed to reflect both differentiation and integration within the thalamocortical system, capturing the rapid and effective interaction (i.e., integration) of functionally specialized modules (i.e., differentiation) [51]. Yet, despite the great advance in application of the PCI to assessing someone's level of consciousness, particularly in complex situations such as patients for whom behavioral responsiveness might be compromised, little is known about the grounding of brain dynamics complexity, as measured by the PCI, and specific aspects of brain architecture. To date, multimodal assessments have only uncovered associations between PCI and global phenotypes typical of disorders of consciousness, such as the degree of residual global brain metabolism (as indexed by FDG-PET) and global white matter structural integrity (as indexed by fractional anisotropy) [53,54]. In light of the known associations between specific cortical and subcortical circuits and depth of DOC impairment [31,32,34,55,56], we perform a novel secondary analysis of previously published data [51,52,57] to explore whether the PCI is related to specific, localized, brain pathology (i.e., cortical ribbon and subcortical atrophy) as opposed to only being a manifestation of global dysfunction [53,54].

## Methods

### Population and procedure

A convenience sample of 40 patients with moderate-to-severe brain injury (29 male, 11 female; mean age = 51.2 years; age SD = 14.2 years) were included in the present analysis, spanning anoxic, traumatic, or vascular etiology (see Table 1 and Fig. 1). Patients were enrolled at three clinical institutions in the greater metropolitan area of Milan, Italy, each equipped with different MRI machines and sequences. At the Neurocritical Care Unit, Department of Neuroscience, ASST Grande Ospedale Metropolitano Niguarda Cà Granda MRI data were recorded on a Philips Achieva 1.5T (sequence GR, TR = 7.632 ms, TE = 3.508 ms, FA = 8°), at Fondazione Europea di Ricerca Biomedica (FERB Onlus) data were recorded on a Philips Achieva 1.5T (sequence GR, TR = 25 ms, TE = 3.684 ms, FA = 30°), while at the IRCCS Fondazione Don Gnocchi data were recorded with a Siemens Avanto 1.5T (sequence GR/IR, TR = 1900 ms, TE = 3.37 ms, FA = 15°). The patients included in this analysis belong to a larger population discussed in previous work [51,52,57] and were selected because, along with PCI measurement, they had a T1-weighted MRI. Importantly, the relationship between subcortical structures and PCI has never been explored in any of the prior work.

As described previously, each patient underwent multiple coma recovery scale revised (CRS-R [58]) assessments for a period of 1 week (4 times, every other day). Patients showing only reflexive behavior across all evaluations were considered as being in a vegetative state (VS), whereas patients showing signs of non-reflexive behaviors in at least 1 evaluation were considered as minimally conscious (MCS; sub-classified as MCS + for patients capable of high-level behavioral responses such as command following and intelligible verbalizations, and MCS- for patients only demonstrating low-level behaviors such as visual pursuit and appropriate contingent behaviors [59]). As conventional, each patient was classified according to highest state demonstrated across the multiple assessments. The TMS/EEG recording session (see Ref. [51] for more detail) was scheduled on the same evaluation week, at least 20 days after DOC onset and 3 days after withdrawal of any sedation. An MRI acquisition (originally acquired for frameless stereotactic guidance) was performed 1–5 days before TMS-EEG in acute patients (i.e., time since injury, TSI < 3 months for anoxic etiology, < 6 months for vascular and traumatic etiology) and 1–30 days before TMS-EEG for chronic patients. To characterize the relationship between PCI and level of consciousness in this sample, we employ a Bayesian ANCOVA analysis framework [60–62], as implemented in JASP (v0.12.2) [63], with PCI as the dependent variable, sex, etiology, and diagnosis as fixed factors, TSI, age, and normalized brain volume (NBV, see below) as covariates. (We note that the results presented below remain qualitatively unchanged if the CRS-R total score is substituted for the categorical diagnosis variable.) Follow-up post-hoc comparison between diagnostic, sex, and etiology groups were also performed and corrected for multiplicity by fixing to 0.5 the prior probability that the null hypothesis holds across all comparisons, thus leading to an adjustment roughly similar to the traditional Bonferroni adjustment of  $p$ -values [64]. The labels used to categorize the strength of the evidence implied by the Bayes Factor (BF) are those presented in Ref. [65]. The Bayesian ANCOVA analysis shows that the subsample employed in this study retains the known link between the highest PCI measurement obtained in a given patient (i.e.,  $\text{PCI}_{\max}$ ) and state of consciousness [48,50,51]. Indeed, compared to the full factorial set of possible models, the model including two main effects, etiology and diagnosis, as well as their interaction, receives the highest empirical support ( $\text{BF}_{10} = 42,810$ ; i.e., the

**Table 1**

**Patient demographic, clinical, and PCI data.** (Abbreviations: Ctr, center; yr, years; M, male; F, female; Etiol, etiology; T, traumatic; V, vascular; A, anoxic; TSI, time since injury; mo, months; Diag, diagnosis; CRS-R, coma recovery scale revised; NBV normalized brain volume; PCI<sub>max</sub>, maximum perturbational complexity index; R, right; L, left; SFG, superior frontal gyrus; SPL, superior parietal lobule. Center 1: Neurocritical Care Unit, Department of Neuroscience, ASST Grande Ospedale Metropolitano Niguarda Cà Granda; center 2: Fondazione Europea di Ricerca Biomedica (FERB Onlus); center 3: IRCCS Fondazione Don Gnocchi.).

ID	Ctr	Age (yr)	Sex	Etiol	TSI (mo)	Diag	CRS-R								NBV (mm <sup>3</sup> )	PCI <sub>max</sub>	Stimulation site providing	Stimulated sites	CRS-R	Arousal during TMS-EEG					
								Auditory	Visual	Motor	Oromotor/Verbal	Communication	Arousal	TOTAL											
01	3	26	F	A	14.00	VS	1	0	1	0	0	0	1	3	1,268,271	0.42	R	SFG	2	1					
02	1	42	M	T	1.00	VS	0	0	1	1	0	0	1	3	1,442,343	0.13	L	SFG	4	1					
03	1	57	M	V	1.00	VS	0	0	1	1	0	0	1	3	1,504,788	0.23	L	SFG	4	1					
04	2	71	M	A	1.30	VS	0	0	2	1	0	0	1	4	1,122,688	0.24	R	SPL	4	1					
05	3	52	M	A	12.70	VS	1	0	0	1	0	0	2	4	1,178,448	0.00			4	2					
06	3	64	M	T	92.80	VS	0	1	1	0	0	0	2	4	1,024,159	0.42	R	SFG	3	2					
07	3	56	M	T	13.10	VS	1	0	1	1	0	0	1	4	1,211,727	0.21	R	SPL	3	1					
08	2	35	M	T	78.00	VS	1	0	2	0	0	0	2	5	1,158,423	0.45	R	SPL	2	2					
09	2	76	F	V	1.20	VS	1	0	2	1	0	0	1	5	1,462,961	0.26	R	SFG	3	1					
10	3	30	M	A	10.30	VS	1	0	2	1	0	0	1	5	1,125,252	0.00			4	1					
11	3	57	M	A	13.30	VS	1	0	2	1	0	0	1	5	1,083,810	0.29	R	SPL	4	1					
12	3	60	M	A	40.20	VS	1	0	1	1	0	0	2	5	1,162,756	0.00			4	2					
13	3	35	M	A	13.60	VS	1	0	2	1	0	0	1	5	1,201,489	0.00			4	1					
14	3	33	M	A	21.80	VS	1	0	1	1	0	0	2	5	1,153,895	0.00			4	2					
15	3	62	M	A	7.20	VS	1	0	2	1	0	0	1	5	1,094,959	0.00			4	1					
16	3	55	M	V	1.60	VS	2	1	0	0	0	0	2	5	1,553,754	0.23	L	SFG	2	1					
17	2	22	M	T	22.30	VS	1	1	1	1	0	0	2	6	1,346,485	0.44	L	SFG	4	2					
18	3	54	M	A	5.90	VS	1	1	1	2	0	0	1	6	1,204,403	0.00			4	1					
19	3	57	M	A	29.40	VS	1	0	2	1	0	0	2	6	1,253,315	0.22	R	SFG	3	2					
20	3	57	F	A	15.70	VS	2	0	2	1	0	0	1	6	1,318,484	0.00			4	1					
21	3	43	F	A	44.90	VS	1	0	2	1	0	0	2	6	1,147,162	0.16	R	SFG	4	2					
22	3	58	M	A	56.50	VS	1	1	2	1	0	0	1	6	1,033,275	0.00			4	1					
23	2	45	M	A	20.20	VS	1	0	2	2	0	0	2	7	1,097,915	0.00			4	2					
24	3	44	F	V	95.00	VS	1	0	2	2	0	0	2	7	1,133,721	0.24	R	SFG	4	2					
25	3	59	F	V	11.90	MCS-	1	3	1	1	0	0	1	7	1,353,768	0.47	R	SPL	4	1					
26	3	32	M	T	29.50	MCS-	2	3	0	1	0	0	1	7	1,479,151	0.27	R	SFG	3	1					
27	3	56	M	V	11.30	MCS-	2	3	1	1	0	0	1	8	1,245,821	0.47	L	SFG	4	1					
28	3	84	F	V	128.40	MCS-	2	3	1	1	0	0	2	9	1,053,172	0.35	R	SFG	3	2					
29	3	61	M	T	50.40	MCS-	2	3	1	1	0	0	2	9	1,273,278	0.36	L	SFG	3	2					
30	3	59	M	A	12.40	MCS-	2	3	1	1	0	0	2	9	1,178,786	0.52	L	SPL	1	2					
31	3	53	F	V	87.60	MCS-	1	3	3	1	0	0	2	10	1,206,527	0.35	R	SPL	3	2					
32	3	24	M	T	33.30	MCS-	2	3	2	1	0	0	2	10	1,362,772	0.53	R	SPL	3	2					
33	2	55	F	V	36.90	MCS-	2	3	2	2	1	0	1	11	1,215,890	0.38	L	SPL	3	1					
34	3	72	M	V	14.30	MCS-	2	3	2	2	0	0	2	11	1,283,898	0.38	L	SPL	4	2					
35	3	55	M	T	11.70	MCS+	0	4	5	2	0	0	2	13	1,341,921	0.41	R	SPL	3	2					
36	3	46	M	A	56.70	MCS+	3	1	4	3	1	0	2	14	1,243,258	0.39	L	SFG	2	2					
37	3	66	F	V	13.20	MCS+	4	0	5	3	1	0	1	14	1,337,973	0.42	L	SPL	4	1					
38	2	43	M	T	10.40	MCS+	3	4	5	1	0	0	2	15	1,451,280	0.36	R	SPL	3	2					
39	3	45	F	V	33.90	MCS+	4	5	5	1	0	0	2	17	1,372,674	0.44	L	SPL	4	2					
40	3	50	M	A	50.10	MCS+	3	5	5	2	1	0	2	18	1,247,936	0.50	L	SPL	3	2					

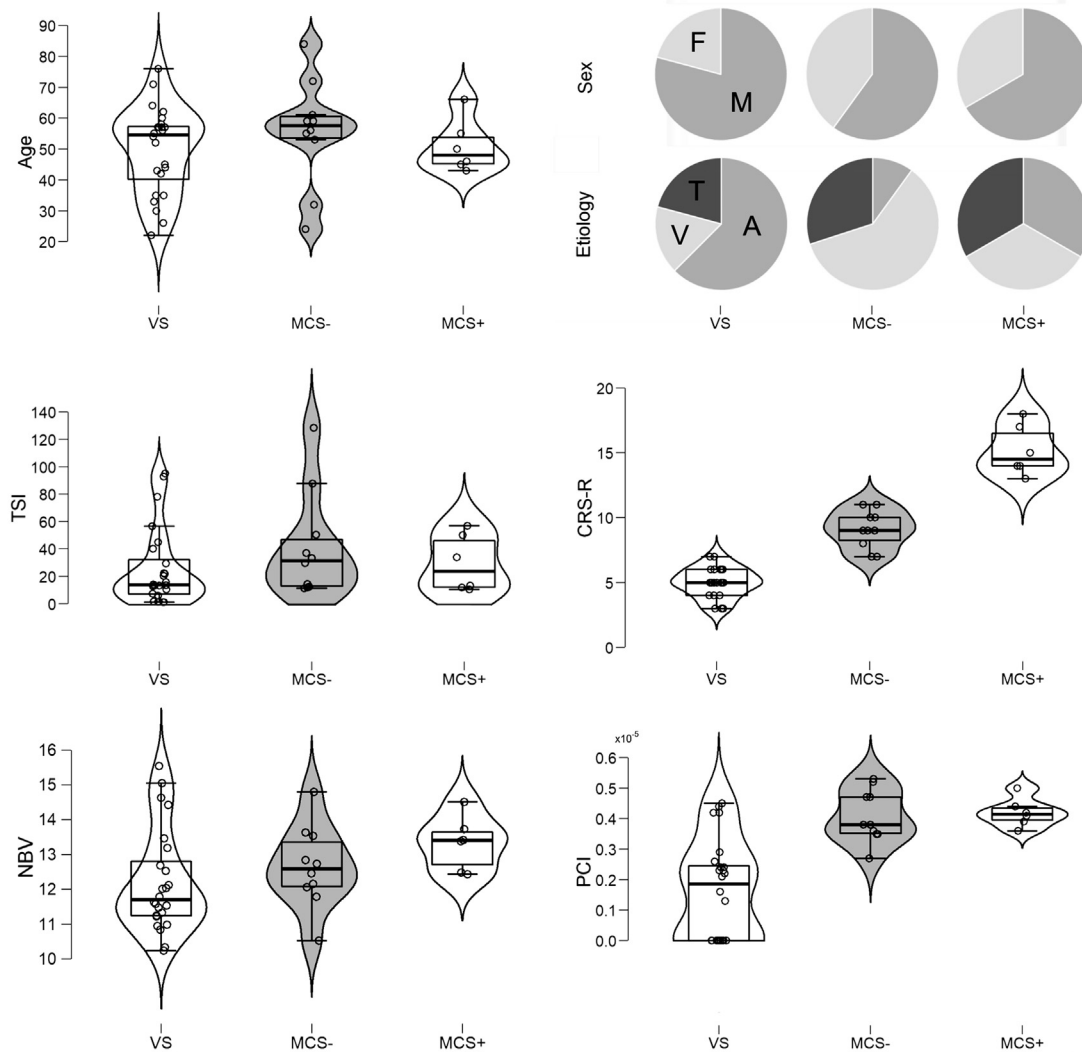


**Fig. 1.** Demographic, clinical, structural and neurophysiological data by diagnosis. (Abbreviations: VS, vegetative state; MCS-/+, minimally conscious state; F, female; M, male; T, traumatic; V, vascular; A, anoxic; TSI, time since injury; CRS-R, coma recovery scale revised; NBV, normalized brain volume; PCI, perturbational complexity index.)

model is almost 43,000 times more likely, as an explanation of the PCI score, than the null model containing only the intercept). In terms of individual predictor variables, consistent with the extant work on PCI in DOC [51,52,57], we unsurprisingly find extreme evidence for diagnosis being associated with PCI (model averaged inclusion Bayes Factor ( $BF_{\text{incl}}$ ) = 176.15). Interestingly, we only find moderate evidence for the interaction of etiology and diagnosis ( $BF_{\text{incl}} = 6.08$ ) and anecdotal evidence for etiology alone ( $BF_{\text{incl}} = 1.98$ ). All other variables (and interactions) were associated with no evidence in favor of a role in explaining PCI (i.e.,  $BF_{\text{incl}} \leq 1$ ). The same model receives extreme support also when compared to a new “null” baseline model including sex, age, TSI, and NBV ( $BF_{10} = 2386.13$ ), resulting in a model averaged  $R^2$  of 0.48 (95% credible interval [0.18 0.70]) as compared to a model averaged  $R^2$  of 0.22 (95% credible interval [0.02 0.42]) when only including sex, age, TSI, and NBV. Post-hoc analyses show that, as expected, the effect of diagnosis on PCI has high posterior odds and very strong

evidence when comparing VS to either MCS group (Posterior odds [ $PO$ ] = 125.21,  $BF_{10,U} = 213.16^1$  and  $PO = 19.89$ ,  $BF_{10,U} = 33.85$ , for MCS- and MCS+ respectively), while there was no evidence in support of a difference between the two MCS groups ( $PO = 0.26$ ,  $BF_{10,U} = 0.45$ ). Post-hoc analyses also show that there is strong evidence in favor of a difference between anoxic etiology and the remaining ones ( $PO = 8.16$ ,  $BF_{10,U} = 13.90$ , and  $PO = 4.54$ ,  $BF_{10,U} = 7.73$ , for vascular and traumatic etiologies, respectively) which, conversely, show no difference ( $PO = 0.23$ ,  $BF_{10,U} = 0.39$ ). (The full JASP result file for this analysis is available at <https://osf.io/tz87j/>.)

#### TMS/EEG procedure and analysis

**TMS-EEG procedure.** TMS-EEG experiments were carried out while patients were behaviorally awake (i.e., eyes-open), using a comprehensive equipment provided by Nexstim Ltd. (Helsinki, Finland). In case of behavioral signs of drowsiness (e.g., eye closure), recordings were momentarily interrupted to apply the CRS-R arousal facilitation protocols [58]. Vigilance was assessed according to the corresponding subscale of the CRS-R and continuously monitored so as to ascertain that the patients always had

<sup>1</sup> It should be noted that in the Bayesian framework, correction for multiplicity applies to the prior odds, as described in the methods section, and not to the BF which, as indicated by the subscript “U,” does not need to be corrected.

their eyes open either spontaneously or with stimulation (see Table 1). EEG data were recorded with a 60-channel TMS-compatible amplifier, referred to an additional electrode on the forehead, band-pass filtered between 0.1 and 350Hz, and sampled at 1,450Hz. TMS was delivered with a focal biphasic stimulator (70-mm diameter) at an intensity equal or greater than 120V/m to maximize the impact of stimulation on the cortical surface. During TMS stimulation, a masking noise was played through in-ear headphones to maximally reduce the contribution of auditory-evoked potentials elicited by TMS-associated clicks. In each patient, several TMS-EEG sessions were collected by stimulating different targets bilaterally within the middle-caudal portion of the superior frontal gyrus (BA6, BA8) and within the superior parietal lobule (BA7) employing a navigated brain stimulation system, which ensured an accurate and reproducible selection of stimulation parameters (site, intensity, angle) on individual anatomical MRIs. TMS over cortical lesions was deliberately avoided because it does not evoke any measurable response [66]. Specifically, 4 sites were stimulated in 22 patients, 3 sites in 13 patients, 2 sites in 4 patients and 1 site in 1 patient. In each TMS-EEG session, at least 150 pulses were delivered.

**TMS-EEG data analysis.** Artifact-contaminated trials and channels were rejected by visual inspection of EEG data. Sessions with more than 10 rejected channels and less than 80 accepted trials were excluded from further analysis. On average,  $175 \pm 56$  (standard deviation) trials per session were accepted across patients (range 80–324). Ocular and muscular artifacts were reduced by Independent Component Analysis. Then, the following automatic pre-processing pipeline was applied to each dataset [50]: 0.1–45Hz band-pass filtering, downsampling at 362.5Hz, estimation of cortical current density, non-parametric statistical analysis to estimate the spatiotemporal pattern of cortical activations significantly evoked by TMS. For each TMS-EEG session, PCI was computed as the Lempel–Ziv complexity of the matrix of significant cortical current density, normalized by the source entropy: this computation resulted in a positive real number ranging between 0 (minimal complexity) and 1 (maximal complexity). PCI was set to 0 when the percentage of spatiotemporal activations surviving statistical analysis was <1% (corresponding to the maximum rate of false positives). Eventually, for each patient, the maximum value of PCI computed across several TMS-EEG sessions ( $\text{PCI}_{\text{max}}$ ) was retained for diagnostic purposes: according to the extensive validation reported in a previous work [51], the  $\text{PCI}_{\text{max}}$  values associated with MCS and VS conditions were respectively higher and lower or equal than 0.31.

#### Subcortical shape analysis

Similarly to our previous work [34,35], structural data were analyzed with a technique referred to as “shape (or vertex) analysis,” as implemented in the FMRIB software library (FSL [67,68], v5.0.9). Specifically, T1-weighted data were first brain-extracted with optiBET [69], a pipeline optimized for the pathological brain shapes typical of patients with severe brain injuries, in order to remove non-brain tissue. Following, we employed FSL FIRST [67] to segment, on a single-subject basis, subcortical structures of interest (i.e., thalamus, caudate nucleus, putamen, globus pallidus, and hippocampus, separately for each hemisphere, and brainstem; see Fig. 2). Each structure was then reconstructed into a 3-dimensional mesh and registered to a cohort average common space employing a multistep algorithm optimized for subcortical registration. This workflow results in the creation of a cohort average subcortical mesh, as well as an image, per each participant, encoding the normal between each vertex for that subject and the cohort average. Negative values of the normal (i.e., inwards displacement

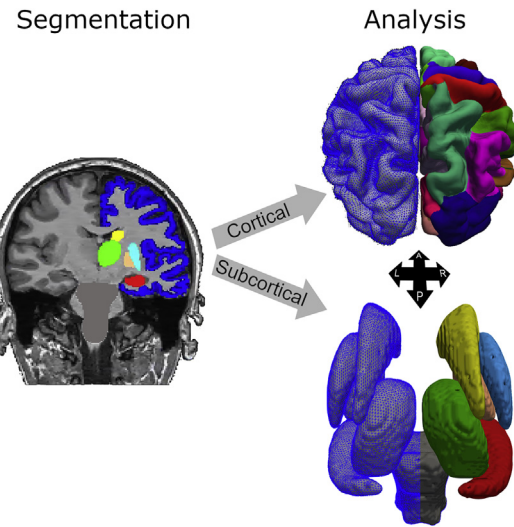


**Fig. 2.** Depiction of the segmentation (left) and 3-dimensional reconstruction of the cortical and subcortical structures of interest (right), highlighting the surface reconstruction (blue mesh) and the ROI subdivisions (one color per ROI). Abbreviations: A, anterior; P, posterior; L, left; R, right. (For interpretation of the references to color in this figure legend, the reader is referred to the Web version of this article.)

of a vertex as compared to the cohort average) can thus be interpreted as marking greater atrophy than average, whereas positive values (i.e., outwards displacement of a vertex as compared to the cohort average) can be interpreted as marking less atrophy than average. In addition to the above preprocessing, we also calculated, for each subject, the normalized brain volume [70]. This measure is included in group analysis to ensure that the results reflect differences in local shape change as opposed to global differences in whole brain atrophy and head size. Prior to any analysis, each segmentation was visually inspected for accuracy with respect to structure boundaries (by ESL) and nine patients were excluded because of poor segmentation quality due to in-scanner motion (seven patients) and low contrast-to-noise and signal-to-noise ratios (two patients; see Table 2 for a breakdown of exclusions by diagnosis and etiology).

#### Cortical thickness analysis

Estimates of cortical ribbon thickness were calculated with Freesurfer (v5.3.0), using the cortical surface stream to construct models of the boundary between white matter and cortical gray matter as well as the pial surface [71,72]. As for the subcortical processing, prior to any analysis, each segmentation was visually inspected for accuracy and 20 patients (encompassing the nine patients for whom subcortical segmentations failed) were excluded because of poor segmentation quality due to in-scanner motion (nine patients), low contrast-to-noise and signal-to-noise ratios (five patients), signal dropout artifact (one patient), and failure to complete the Freesurfer workflow (five patients) (see Table 2). For the remaining cases, group analyses were performed on a cohort-specific average template, which facilitates registration of severely damaged brains and allows removing pose and global scaling across different scanners.

#### Statistical analysis

Group effects were estimated with a general linear model approach including the estimated cross-sectional cortical and subcortical measures as the dependent variable (i.e., the per-vertex

**Table 2**

Detail of patient exclusions by diagnosis and etiology.

	Subcortical analysis		Cortical analysis	
	Included (n = 31)	Excluded (n = 9)	Included (n = 20)	Excluded (n = 20)
MCS+	5	1	6	0
MCS-	7	3	4	6
VS	19	5	10	14
Traumatic	9	1	5	5
Vascular	8	4	7	5
Anoxic	14	4	8	10

normals, for subcortical data, and per-voxel ribbon thickness estimate, for cortical data), and PCI score, sex, days post injury, age, etiology, and NBV as predictor variables. Significance of estimated vertex-/voxel-wise statistics was assessed with a non-parametric permutation approach (with FSL randomise [73] for the subcortex and Freesurfer mri\_glmfit-sim –perm [74–76] for the cortex) at a criterion of  $p = 0.05$  corrected for multiple comparisons with a family-wise cluster correction and threshold-free cluster enhancement for the subcortex (TFCE; see Ref. [77]).

## Results

As depicted in Fig. 3 (see also eTable 1),  $\text{PCI}_{\max}$  scores were negatively associated with atrophy in the bilateral globus pallidus (GP) ( $T = 3.34$ ,  $p = 0.012$ , and  $T = 3.82$ ,  $p = 0.017$ , for right and left hemispheres, respectively), with 91% and 79% of GP vertices showing a significant association with the maximum complexity score, for right and left hemispheres respectively. While our technique does not segment separately the external (GPe) and internal (GPi) segments of the globus pallidus, according to atlas-based coordinates, 73% of the atrophy is in GPe (78% left, 70% right), and 27% of the atrophy is in the GPi (22% left, 30% right). In addition, left caudate was also significantly associated, negatively, with  $\text{PCI}_{\max}$  ( $T = 4.55$ ,  $p = 0.042$ ) but only in a small antero-medial area of the structure (i.e., 4%). These results persist (qualitatively) with or without the inclusion of age, TSI, sex, T1-weighted MRI acquisition protocol, and normalized brain volume covariates. Inclusion of etiology, however, resulted in the right GP ( $T = 3.80$ ,  $p = 0.012$ ) and left caudate ( $T = 6.92$ ,  $p = 0.034$ ) remaining significantly associated with PCI, in 89% and 8.4% of vertices respectively, whereas the left GP cluster no longer showed such an association ( $p = 0.08$ ), implying shared variance with etiology (see eFig. 1). The presence of shared variance between the two variables is unsurprising considering their significant association ( $\text{BF}_{10} = 45.30$ ) owing to the greater proportion of VS patients with anoxic etiology (see Fig. 1). Etiology, however, was found to have no significant association with subcortical atrophy. Time since injury was negatively associated with subcortical atrophy in small regions of the brainstem ( $T = 4.64$ ,  $p = 0.05$ ; <1% of vertices), left hippocampus ( $T = 5.41$ ,  $p = 0.027$ ; 12% of vertices), and right putamen ( $T = 3.93$ ,  $p = 0.049$ ; 2.6% of vertices) (see eFig. 1).

Finally, the cortical analysis did not reveal any significant association between ribbon thinning and  $\text{PCI}_{\max}$ .

## Discussion

Over the last 15 years, the realization of the logical shortcomings of behavior-based approaches to assessing someone's level of consciousness has motivated a large research effort aimed at devising novel strategies for correctly discriminating conscious (if minimally) from unconscious patients on the basis of brain activity alone – be it voluntary [18,78] or spontaneous [27,31]. One theory-based approach, in particular, the so-called perturbational

complexity index [50], is emerging as a technique which combines the benefits of passive approaches, that is, being agnostic and robust to a patient's level of residual cognitive functioning, while also offering, *vis-à-vis* extensive benchmarking [51], a level of simple single-patient actionable information (i.e., conscious/unconscious) more typical of active paradigms.

In the present work, we take advantage of previous data to perform a novel analysis aimed at searching for structural correlates of the TMS/EEG-derived measure of brain integration and differentiation (i.e., PCI). Overall, we find that atrophy in the globus pallidus to be inversely associated with the emergence of the brain-wide distributed interactions measured by the PCI. The globus pallidus has been associated with electro-cortical and/or behavioral arousal across animal models [79–82], healthy volunteers [25], and patient studies [34]. Indeed, this region is believed to have efferent connections to sensory/motor (its internal segment) and frontal cortices (its external segment [83,84]), a geometry which could allow it to broadly influence behavioral and electrocortical arousal. In the rodent model, cell body-specific lesions of the globus pallidus (i.e., the human correlative of the pars externa) using ibotenic acid alters the sleep-wake cycle and leads to a shift of electroencephalographic power towards slow (i.e., delta) frequencies [85]. In healthy volunteers, the loss and restoration of pallido-cortical connectivity was associated with loss and recovery of consciousness in the anesthetic model [25]. In a large cohort of DOC patients, atrophy in the globus pallidus has been associated with decreased behavioral arousal [34], mirroring the association between abnormal pallidal function in patients with Parkinson's disease [86–90] and sleep-related symptomatology [91–95]. Furthermore, the globus pallidus is currently believed to be a key mediator of the arousing effect of zolpidem on patients with disorders of consciousness [55,96]. Although speculative, it is thus possible that the previously reported association between pallidal atrophy and decreased behavioral arousal [34] might be mediated by this region's role in maintaining an optimal equilibrium between excitatory and inhibitory drives that are necessary for the emergence of complex pattern of causal interactions among cortical neurons [52]. This interpretation is also consistent with recent data associating pallidal atrophy with slowing of the spectrum at rest (i.e., beta/delta ratio) in chronic DOC [97]. However, despite the growing interest in the non-motor related functions of this nucleus [82], its intricate pattern of connections, collaterals, and reciprocal innervations (e.g. Ref. [98]), the balance of complex intrinsic pace-making conductances, different neurotransmitters (i.e., glutamate and GABA), and rich variety of cell subpopulations and receptor subtypes [99,100], as well as their complex patterns of subregional [101,102], subcellular, and subsynaptic (co)localization [103], make it difficult to infer from the level of resolution of a T1-weighted MR image the specific mechanism by which widespread bilateral pallidal atrophy might lead to the brain-wide disruption of causal interactions as measured by the PCI. Still, this complex underlying architecture hints at the globus pallidus (and its external segment in particular) playing an important role in modulating, both in time and in space, the neural information that flows through the

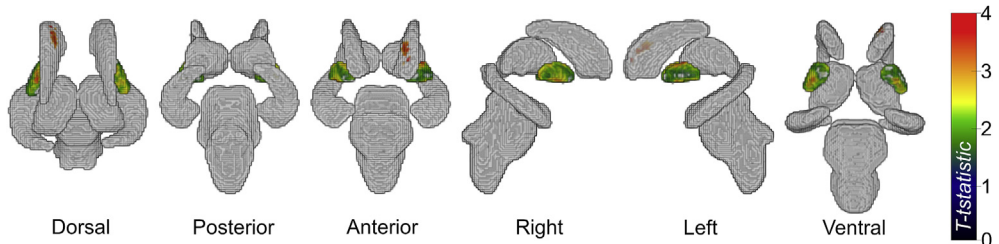


**Fig. 3.** Shape analysis results depicting regions where greater atrophy is significantly, and inversely, associated with  $\text{PCI}_{\max}$ . (Areas in gray indicate no significant association between vertex normal and PCI. Bilateral putamen removed for display only.)

basal ganglia [98,104], a key circuit also in the context of loss and recovery of consciousness after severe brain injury [55]. We also note that while we find bilateral association between GP and PCI, the right GP atrophy appears to be a common denominator across types of brain injuries, whereas the left GP appears to share variance with etiology. The significance of this lateralization remains to be understood.

The association between PCI, an index sensitive to the presence of consciousness, and the globus pallidus, a structure important for electrocortical arousal and sleep-wake behavior, highlights an under-acknowledged gap in a definitional component of disorders of consciousness [3]. According to international guidelines, VS and MCS patients are equally characterized by the return of periods of arousal (behaviorally defined) [3,105]. Yet, differences in physiological indicators of circadian rhythms [106–108] and electrocortical arousal [109–111] across the two groups have been well characterized, with clearer sleep-wake cycles and greater electrocortical arousal being associated preferentially with MCS patients. Furthermore, prior work shows that PCI decreases gradually in the process of falling asleep (from wakefulness to N1 and N3 [50]) and that the build-up of complexity is hampered by the occurrence of sleep-like dynamics (i.e., OFF-periods), as observed in sleeping volunteers and brain injury patients [52], as well as cortical slices [112], that are in turn typically engendered by decreased level of neuromodulation. So it is not surprising that aspects of brain function tied to arousal differ across VS and MCS patients even though their behaviorally defined arousal phenotype is similar. In fact, the present findings call further attention to the need for a better characterization of arousal in disorders of consciousness beyond simple observation of eye-opening [108].

Beyond the GP, we also find a small region of negative association between atrophy in the left caudate and PCI. This region is considered to be part of the mesocircuit underlying brain dysfunction in DOC [55], and stimulation of the caudate head has been shown to suppress cortical excitability [113], while lesions in this area have been associated with hyperarousal in animal models [114] and hyperactivity and restlessness in human patients [115]. Nonetheless, the very small size of the association between PCI and caudate (4% of its extent) and the well-known associations between caudate and other motor and cognitive symptomatology [115] urge caution in interpreting this result.

Finally, it is noteworthy that in our sample we fail to find a correlation between thalamus and PCI; for, prior work has shown that thalamic lesions are associated with modulation of cortical excitability [116–118].

Overall, our findings match the previously reported associations between global phenotypes typical of DOC, such as broadly decreased metabolism and loss of global white matter integrity, and PCI [53,54]. Here, however, we show for the first time that the relationship between the causal brain interactions captured by the PCI and brain structure is also sensitive to localized brain pathology

in a region considered to be key for behavioral and electrocortical function in both animal models [79–82,85] and in human patient populations, including DOC [34,35,88–90].

In assessing these results, the reader should be mindful of some limitations. First, segmentation of brain regions is notoriously difficult to perform in the presence of pathological shapes typical of severe brain-injury cohorts. Here, we have mitigated this issue by employing previously developed and validated tools (more) robust to pathological brain shapes than other available software (i.e., optiBET [69]), co-registration algorithms optimized for subcortical structures (first\_flirt, FSL [68]), and visual inspection. Second, our convenience sample includes patients at very different time post-injury, from sub-acute (i.e., 1 month post-injury) to very chronic (i.e., 10 years post-injury; cf., Table 1 and Fig. 1). While there is reason to believe that, at least as assessed with MRI, the pattern of chronic atrophy typical of DOC (e.g. Ref. [34]) is already set within the first six months post injury [35,56,119], we took the standard approach of simply partialing out this variable. Third, while our shape analysis is advantageous in that it makes use of conventional data routinely acquired in the clinic (i.e., a T1-weighted MRI), it is blind to the finer detail of cellular populations, different firing patterns, neurotransmitter affinity, and receptor distribution, variables that are likely to play an important role in the relationship between post-brain injury pathology and the neurophysiological signal the analysis is based upon. Finally, we stress that it is difficult to interpret the null finding generated from the cortical analysis. For, we are unable to tell whether it is due to a genuine lack of association between cortical thickness and PCI, because of excessive variance in the pattern of cortical injury across our sample, or whether it is simply due to lack of power because of the exclusion, due to segmentation quality, of a large proportion of the initial sample.

In conclusion, in the present work, we describe for the first time the patterns of association between a global measure of brain complexity [50], and specific, localized, aspects of brain pathology (i.e., atrophy) after severe brain injury. Furthermore, these results suggest that the reported association between pallidal atrophy, slowing of EEG frequency [97], and low arousal in chronic DOC patients [34] might be mediated by the involvement of the globus pallidus in maintaining a critical electrocortical balance between excitation and inhibition necessary for the emergence of complex cortical dynamics [52]. These findings add a new layer to our understanding of the neural mechanisms that support a state of consciousness and provide new information that could be leveraged for developing novel therapeutic interventions in patients suffering from disorders of consciousness [120,121].

#### CRediT authorship contribution statement

**Evan S. Lutkenhoff:** Methodology, Software, Validation, Formal analysis, Writing - original draft, Visualization. **Micah A. Johnson:**

**Methodology, Software, Writing - review & editing.** **Silvia Casarotto:** Methodology, Investigation, Resources, Data curation, Writing - review & editing. **Marcello Massimini:** Conceptualization, Writing - review & editing, Supervision, Project administration, Funding acquisition. **Martin M. Monti:** Conceptualization, Writing - original draft, Visualization, Supervision, Project administration, Funding acquisition.

## Acknowledgments

This work was funded in part by the Tiny Blue Dot Foundation (M.M.M.), European Union's Horizon 2020 Framework Program for Research and Innovation under the Specific Grant Agreement No. 785907 (Human Brain Project SGA2) (to M.M.) and by the EU grant H2020, FETOPEN 2014-2015-RIA no. 686764 "Luminous" (to M.M.).

The authors have no financial interest to disclose.

## Appendix A. Supplementary data

Supplementary data to this article can be found online at <https://doi.org/10.1016/j.brs.2020.07.012>.

## References

- [1] Monti MM, Coleman MR, Owen AM. Neuroimaging and the vegetative state: resolving the behavioral assessment dilemma? *Ann N Y Acad Sci* 2009;1157(1):81–9.
- [2] Owen AM, Coleman MR. Functional neuroimaging of the vegetative state. *Nat Rev Neurosci* 2008;9(3):235–43.
- [3] Laureys S. The neural correlate of (un)awareness: lessons from the vegetative state. *Trends Cognit Sci* 2005;9(12):556–9.
- [4] Monti MM. Cognition in the vegetative state. *Annu Rev Clin Psychol* 2012;8: 431–54.
- [5] Monti MM, Owen AM. Behavior in the brain using functional neuroimaging to assess residual cognition and awareness after severe brain injury. *J Psychophysiol* 2010;24(2):76–82.
- [6] Childs NL, Mercer WN. Misdiagnosing the persistent vegetative state. Misdiagnosis certainly occurs. *BMJ* 1996;313(7062):944.
- [7] Childs NL, Mercer WN, Childs HW. Accuracy of diagnosis of persistent vegetative state. *Neurology* 1993;43(8):1465–7.
- [8] Gill-Thwaites H. Lotteries, loopholes and luck: misdiagnosis in the vegetative state patient. *Brain Inj* 2006;20(13–14):1321–8.
- [9] Schnakers C, Giacino J, Kalmar K, Piret S, Lopez E. Does the FOUR score correctly diagnose the vegetative and minimally conscious states? tomographic visualization of cholinesterase. *Ann Neurol* 2006;60(6):2005–6.
- [10] Schnakers C, Vanhaudenhuyse A, Giacino J, Ventura M, Boly M, Majerus S, et al. Diagnostic accuracy of the vegetative and minimally conscious state: clinical consensus versus standardized neurobehavioral assessment. *BMC Neurol* 2009;9:35.
- [11] Fins JJ, Schiff ND. Shades of gray: new insights into the vegetative state. *Hastings Cent Rep* 2006;36(6):8.
- [12] Jennett B. The vegetative state: medical facts, ethical and legal dilemmas. Cambridge Univ Press; 2002.
- [13] Monti MM, Pickard JD, Owen AM. Visual cognition in disorders of consciousness: from V1 to top-down attention. *Hum Brain Mapp* 2013;34(6): 1245–53.
- [14] Bardin JC, Fins JJ, Katz DI, Hersh J, Heier LA, Tabelow K, et al. Dissociations between behavioural and functional magnetic resonance imaging-based evaluations of cognitive function after brain injury. *Brain* 2011;134(Pt 3): 769–82.
- [15] Chennu S, Finoia P, Kamau E, Monti MM, Allanson J, Pickard JD, et al. Dissociable endogenous and exogenous attention in disorders of consciousness. *Neuroimage Clin* 2013;3:450–61.
- [16] Naci L, Owen AM. Making every word count for nonresponsive patients. *JAMA Neurol* 2013;70(10):1235–41.
- [17] Monti MM, Rosenberg M, Finoia P, Kamau E, Pickard JD, Owen AM. Thalamofrontal connectivity mediates top-down cognitive functions in disorders of consciousness. *Neurology* 2015;84(2):167–73.
- [18] Owen AM, Coleman MR, Boly M, Davis MH, Laureys S, Pickard JD. Detecting awareness in the vegetative state. *Science* 2006;313(5792):1402.
- [19] Schnakers C, Perrin F, Schabus M, Majerus S, Ledoux D, Damas P, et al. Voluntary brain processing in disorders of consciousness. *Neurology* 2008;71(20):1614–20.
- [20] Stender J, Gosseries O, Bruno MA, Charland-Verville V, Vanhaudenhuyse A, Demertzi A, et al. Diagnostic precision of PET imaging and functional MRI in disorders of consciousness: a clinical validation study. *Lancet* 2014;384(9942):514–22.
- [21] Lutkenhoff ES, Monti MM. Brain responsiveness after severe brain injury: revolutions and controversies. *Brain function and responsiveness in disorders of consciousness*. Springer; 2016. p. 81–92.
- [22] Chennu S, Finoia P, Kamau E, Allanson J, Williams GB, Monti MM, et al. Spectral signatures of reorganized brain networks in disorders of consciousness. *PLoS Comput Biol* 2014;10(10):e1003887.
- [23] Fernandez-Espejo D, Soddu A, Cruse D, Palacios EM, Junque C, Vanhaudenhuyse A, et al. A role for the default mode network in the bases of disorders of consciousness. *Ann Neurol* 2012;72(3):335–43.
- [24] Crone JS, Bio BJ, Vespa PM, Lutkenhoff ES, Monti MM. Restoration of thalamo-cortical connectivity after brain injury: recovery of consciousness, complex behavior, or passage of time? *J Neurosci Res* 2018;96(4):671–87.
- [25] Crone JS, Lutkenhoff ES, Bio BJ, Laureys S, Monti MM. Testing proposed neuronal models of effective connectivity within the cortico-basal ganglia-thalamo-cortical loop during loss of consciousness. *Cerebr Cortex* 2017;27(4):2727–38.
- [26] Crone JS, Schurz M, Holler Y, Bergmann J, Monti M, Schmid E, et al. Impaired consciousness is linked to changes in effective connectivity of the posterior cingulate cortex within the default mode network. *Neuroimage* 2015;110: 101–9.
- [27] Demertzi A, Tagliazucchi E, Dehaene S, Deco G, Barttfeld P, Raimondo F, et al. Human consciousness is supported by dynamic complex patterns of brain signal coordination. *Sci Adv* 2019;5(2):eaat7603.
- [28] Monti MM, Lutkenhoff ES, Rubinov M, Boveroux P, Vanhaudenhuyse A, Gosseries O, et al. Dynamic change of global and local information processing in propofol-induced loss and recovery of consciousness. *PLoS Comput Biol* 2013;9(10):e1003271.
- [29] Rosazza C, Andronache A, Sattin D, Bruzzone MG, Marotta G, Nigri A, et al. Multimodal study of default-mode network integrity in disorders of consciousness. *Ann Neurol* 2016;79(5):841–53.
- [30] Soddu A, Vanhaudenhuyse A, Bahri MA, Bruno MA, Boly M, Demertzi A, et al. Identifying the default-mode component in spatial IC analyses of patients with disorders of consciousness. *Hum Brain Mapp* 2012;33(4):778–96.
- [31] Vanhaudenhuyse A, Noirhomme Q, Tshibanda LJ, Bruno MA, Boveroux P, Schnakers C, et al. Default network connectivity reflects the level of consciousness in non-communicative brain-damaged patients. *Brain* 2010;133(Pt 1):161–71.
- [32] Fernandez-Espejo D, Bekinschtein T, Monti MM, Pickard JD, Junque C, Coleman MR, et al. Diffusion weighted imaging distinguishes the vegetative state from the minimally conscious state. *Neuroimage* 2011;54(1):103–12.
- [33] Fernandez-Espejo D, Junque C, Bernabeu M, Roig-Rovira T, Vendrell P, Mercader JM. Reductions of thalamic volume and regional shape changes in the vegetative and the minimally conscious states. *J Neurotrauma* 2010;27(7):1187–93.
- [34] Lutkenhoff ES, Chiang J, Tshibanda L, Kamau E, Kirsch M, Pickard JD, et al. Thalamic and extrathalamic mechanisms of consciousness after severe brain injury. *Ann Neurol* 2015;78(1):68–76.
- [35] Schnakers C, Lutkenhoff ES, Bio BJ, McArthur DL, Vespa PM, Monti MM. Acute EEG spectra characteristics predict thalamic atrophy after severe TBI. *J Neurol Neurosurg Psychiatry* 2019;90(5):617–9.
- [36] Boly M, Faymonville ME, Peigneux P, Lambertz B, Damas P, Del Fiore G, et al. Auditory processing in severely brain injured patients: differences between the minimally conscious state and the persistent vegetative state. *Arch Neurol* 2004;61(2):233–8.
- [37] Boly M, Faymonville ME, Schnakers C, Peigneux P, Lambertz B, Phillips C, et al. Perception of pain in the minimally conscious state with PET activation: an observational study. *Lancet Neurol* 2008;7(11):1013–20.
- [38] Coleman MR, Davis MH, Rodd JM, Robson T, Ali A, Owen AM, et al. Towards the routine use of brain imaging to aid the clinical diagnosis of disorders of consciousness. *Brain* 2009;132(Pt 9):2541–52.
- [39] Coleman MR, Rodd JM, Davis MH, Johnsrude IS, Menon DK, Pickard JD, et al. Do vegetative patients retain aspects of language comprehension? Evidence from fMRI. *Brain* 2007;130(10):2494–507.
- [40] Laureys S, Faymonville ME, Peigneux P, Damas P, Lambertz B, Del Fiore G, et al. Cortical processing of noxious somatosensory stimuli in the persistent vegetative state. *Neuroimage* 2002;17(2):732–41.
- [41] Nigri A, Catricala E, Ferraro S, Bruzzone MG, D'Incerti L, Sattin D, et al. The neural correlates of lexical processing in disorders of consciousness. *Brain Imaging Behav* 2017;11(5):1526–37.
- [42] Owen AM, Menon DK, Johnsrude IS, Bor D, Scott SK, Manly T, et al. Detecting residual cognitive function in persistent vegetative state. *Neurocase* 2002;8(5):394–403.
- [43] Annen J, Frasso G, Crone JS, Heine I, Di Perri C, Martial C, et al. Regional brain volumetry and brain function in severely brain-injured patients. *Ann Neurol* 2018;83(4):842–53.
- [44] Demertzi A, Antonopoulos G, Heine I, Voss HU, Crone JS, de Los Angeles C, et al. Intrinsic functional connectivity differentiates minimally conscious from unresponsive patients. *Brain* 2015;138(Pt 9):2619–31.
- [45] Engemann DA, Raimondo F, King JR, Rohaut B, Louppe G, Faugeras F, et al. Robust EEG-based cross-site and cross-protocol classification of states of consciousness. *Brain* 2018;141(11):3179–92.
- [46] Boly M, Massimini M, Tononi G. Theoretical approaches to the diagnosis of altered states of consciousness. *Prog Brain Res* 2009;177(C):383–98.

- [47] Massimini M, Ferrarelli F, Huber R, Esser SK, Singh H, Tononi G. Breakdown of cortical effective connectivity during sleep. *Science* 2005;309(5744):2228–32.
- [48] Rosanova M, Gosseries O, Casarotto S, Boly M, Casali AG, Bruno MA, et al. Recovery of cortical effective connectivity and recovery of consciousness in vegetative patients. *Brain* 2012;135(Pt 4):1308–20.
- [49] Massimini M, Tononi G. Sizing up consciousness : towards an objective measure of the capacity for experience. first ed. Oxford, United Kingdom: Oxford University Press; 2018.
- [50] Casali AG, Gosseries O, Rosanova M, Boly M, Sarasso S, Casali KR, et al. A theoretically based index of consciousness independent of sensory processing and behavior. *Sci Transl Med* 2013;5(198):198ra05.
- [51] Casarotto S, Comanducci A, Rosanova M, Sarasso S, Fecchio M, Napolitani M, et al. Stratification of unresponsive patients by an independently validated index of brain complexity. *Ann Neurol* 2016;80(5):718–29.
- [52] Rosanova M, Fecchio M, Casarotto S, Sarasso S, Casali AG, Pigorini A, et al. Sleep-like cortical OFF-periods disrupt causality and complexity in the brain of unresponsive wakefulness syndrome patients. *Nat Commun* 2018;9(1):4427.
- [53] Bodart O, Amico E, Gomez F, Casali AG, Wannez S, Heine L, et al. Global structural integrity and effective connectivity in patients with disorders of consciousness. *Brain Stimul* 2018;11(2):358–65.
- [54] Bodart O, Gosseries O, Wannez S, Thibaut A, Annen J, Boly M, et al. Measures of metabolism and complexity in the brain of patients with disorders of consciousness. *Neuroimage Clin* 2017;14:354–62.
- [55] Schiff ND. Recovery of consciousness after brain injury: a mesocircuit hypothesis. *Trends Neurosci* 2010;33(1):1–9.
- [56] Lutkenhoff ES, McArthur DL, Hua X, Thompson PM, Vespa PM, Monti MM. Thalamic atrophy in antero-medial and dorsal nuclei correlates with six-month outcome after severe brain injury. *Neuroimage Clin* 2013;3:396–404.
- [57] Comolatti R, Pigorini A, Casarotto S, Fecchio M, Faria G, Sarasso S, et al. A fast and general method to empirically estimate the complexity of brain responses to transcranial and intracranial stimulations. *Brain Stimul* 2019;12(5):1280–9.
- [58] Giacino JT, Kalmar K, Whyte J. The JFK Coma Recovery Scale-Revised: measurement characteristics and diagnostic utility. *Arch Phys Med Rehabil* 2004;85(12):2020–9.
- [59] Bruno MA, Vanhaudenhuyse A, Thibaut A, Moonen G, Laureys S. From unresponsive wakefulness to minimally conscious PLUS and functional locked-in syndromes: recent advances in our understanding of disorders of consciousness. *J Neurol* 2011;258(7):1373–84.
- [60] Rouder JN, Engelhardt CR, McCabe S, Morey RD. Model comparison in ANOVA. *Psychon Bull Rev* 2016;23(6):1779–86.
- [61] Rouder JN, Morey RD, Speckman PL, Province JM. Default Bayes factors for ANOVA designs. *J Math Psychol* 2012;56(5):356–74.
- [62] Rouder JN, Morey RD, Verhagen J, Swagman AR, Wagenmakers EJ. Bayesian analysis of factorial designs. *Psychol Methods* 2017;22(2):304–21.
- [63] JASP Team. JASP (version 0.9)[computer software]. Amsterdam, NLD: University of Amsterdam; 2018.
- [64] Westfall PH, Johnson WO, Utts JM. A Bayesian perspective on the Bonferroni adjustment. *Biometrika* 1997;84(2):419–27.
- [65] Wagenmakers EJ, Love J, Marsman M, Jamil T, Ly A, Verhagen J, et al. Bayesian inference for psychology. Part II: example applications with JASP. *Psychon Bull Rev* 2018;25(1):58–76.
- [66] Gosseries O, Sarasso S, Casarotto S, Boly M, Schnakers C, Napolitani M, et al. On the cerebral origin of EEG responses to TMS: insights from severe cortical lesions. *Brain Stimul* 2015;8(1):142–9.
- [67] Patenaude B, Smith SM, Kennedy DN, Jenkinson M. A Bayesian model of shape and appearance for subcortical brain segmentation. *Neuroimage* 2011;56(3):907–22.
- [68] Smith SM, Jenkinson M, Woolrich MW, Beckmann CF, Behrens TE, Johansen-Berg H, et al. Advances in functional and structural MR image analysis and implementation as FSL. *Neuroimage* 2004;23(Suppl 1):S208–19.
- [69] Lutkenhoff ES, Rosenberg M, Chiang J, Zhang K, Pickard JD, Owen AM, et al. Optimized brain extraction for pathological brains (optiBET). *PloS One* 2014;9(12):e115551.
- [70] Smith SM, Zhang Y, Jenkinson M, Chen J, Matthews PM, Federico A, et al. Accurate, robust, and automated longitudinal and cross-sectional brain change analysis. *Neuroimage* 2002;17(1):479–89.
- [71] Dale AM, Fischl B, Sereno MI. Cortical surface-based analysis. I. Segmentation and surface reconstruction. *Neuroimage* 1999;9(2):179–94.
- [72] Fischl B, Sereno MI, Dale AM. Cortical surface-based analysis. II: inflation, flattening, and a surface-based coordinate system. *Neuroimage* 1999;9(2):195–207.
- [73] Winkler AM, Ridgway GR, Webster MA, Smith SM, Nichols TE. Permutation inference for the general linear model. *Neuroimage* 2014;92:381–97.
- [74] Greve DN, Fischl B. False positive rates in surface-based anatomical analysis. *Neuroimage* 2018;171:6–14.
- [75] Hayasaka S, Nichols TE. Validating cluster size inference: random field and permutation methods. *Neuroimage* 2003;20(4):2343–56.
- [76] Nichols TE, Holmes AP. Nonparametric permutation tests for functional neuroimaging: a primer with examples. *Hum Brain Mapp* 2002;15(1):1–25.
- [77] Smith SM, Nichols TE. Threshold-free cluster enhancement: addressing problems of smoothing, threshold dependence and localisation in cluster inference. *Neuroimage* 2009;44(1):83–98.
- [78] Monti MM, Vanhaudenhuyse A, Coleman MR, Boly M, Pickard JD, Tshibanda L, et al. Willful modulation of brain activity in disorders of consciousness. *N Engl J Med* 2010;362(7):579–89.
- [79] Qiu MH, Chen MC, Wu J, Nelson D, Lu J. Deep brain stimulation in the globus pallidus externa promotes sleep. *Neuroscience* 2016;322:115–20.
- [80] Qiu MH, Vetrivelan R, Fuller PM, Lu J. Basal ganglia control of sleep-wake behavior and cortical activation. *Eur J Neurosci* 2010;31(3):499–507.
- [81] Qiu MH, Yao QL, Vetrivelan R, Chen MC, Lu J. Nigrostriatal dopamine acting on globus pallidus regulates sleep. *Cerebr Cortex* 2016;26(4):1430–9.
- [82] Lazarus M, Huang ZL, Lu J, Urade Y, Chen JF. How do the basal ganglia regulate sleep-wake behavior? *Trends Neurosci* 2012;35(12):723–32.
- [83] Saunders A, Oldenburg IA, Berezovskii VK, Johnson CA, Kingery ND, Elliott HL, et al. A direct GABAergic output from the basal ganglia to frontal cortex. *Nature* 2015;521(7550):85–9.
- [84] Zheng ZS, Monti MM. Thalamic and extra-thalamic connections of the Globus Pallidus in the human brain: the ultradirect pathway. *bioRxiv* 2019: 688283. <https://doi.org/10.1101/688283>.
- [85] Vetrivelan R, Qiu MH, Chang C, Lu J. Role of Basal Ganglia in sleep-wake regulation: neural circuitry and clinical significance. *Front Neuroanat* 2010;4:145.
- [86] Bevan MD, Magill PJ, Terman D, Bolam JP, Wilson CJ. Move to the rhythm: oscillations in the subthalamic nucleus-external globus pallidus network. *Trends Neurosci* 2002;25(10):525–31.
- [87] Gatev P, Darbin O, Wichmann T. Oscillations in the basal ganglia under normal conditions and in movement disorders. *Mov Disord* 2006;21(10):1566–77.
- [88] Hutchison WD, Lozano AM, Davis KD, Saint-Cyr JA, Lang AE, Dostrovsky JO. Differential neuronal activity in segments of globus pallidus in Parkinson's disease patients. *Neuroreport* 1994;5(12):1533–7.
- [89] Magnin M, Morel A, Jeanmonod D. Single-unit analysis of the pallidum, thalamus and subthalamic nucleus in parkinsonian patients. *Neuroscience* 2000;96(3):549–64.
- [90] Mallet N, Pogosyan A, Marton LF, Bolam JP, Brown P, Magill PJ. Parkinsonian beta oscillations in the external globus pallidus and their relationship with subthalamic nucleus activity. *J Neurosci* 2008;28(52):14245–58.
- [91] Chaudhuri KR, Healy DG, Schapira AH, National Institute for Clinical E. Non-motor symptoms of Parkinson's disease: diagnosis and management. *Lancet Neurol* 2006;5(3):235–45.
- [92] Garcia-Borreguero D, Larrosa O, Bravo M. Parkinson's disease and sleep. *Sleep Med Rev* 2003;7(2):115–29.
- [93] Juri C, Chana P, Tapia J, Kunstmann C, Parrao T. Quetiapine for insomnia in Parkinson disease: results from an open-label trial. *Clin Neuropharmacol* 2005;28(4):185–7.
- [94] Partinen M. Sleep disorder related to Parkinson's disease. *J Neurol* 1997;244(4 Suppl 1):S3–6.
- [95] Trenkwalder C. Sleep dysfunction in Parkinson's disease. *Clin Neurosci* 1998;5(2):107–14.
- [96] Brefel-Courbon C, Payoux P, Ory F, Sommet A, Slaoui T, Raboyeau G, et al. Clinical and imaging evidence of zolpidem effect in hypoxic encephalopathy. *Ann Neurol* 2007;62(1):102–5.
- [97] Lutkenhoff ES, Nigri A, Sebastianiano DR, Sattin D, Visani E, Rosazza C, et al. EEG power spectra and subcortical pathology in chronic disorders of consciousness. *bioRxiv* 2019:695288.
- [98] Sato F, Lavallee P, Levesque M, Parent A. Single-axon tracing study of neurons of the external segment of the globus pallidus in primate. *J Comp Neurol* 2000;417(1):17–31.
- [99] Jaeger D, Kita H. Functional connectivity and integrative properties of globus pallidus neurons. *Neuroscience* 2011;198:44–53.
- [100] Kita H. Globus pallidus external segment. *Prog Brain Res* 2007;160:111–33.
- [101] Boyes J, Bolam JP. Localization of GABA receptors in the basal ganglia. *Prog Brain Res* 2007;160:229–43.
- [102] Waldvogel HJ, Billinton A, White JH, Emson PC, Faull RL. Comparative cellular distribution of GABA<sub>A</sub> and GABA<sub>B</sub> receptors in the human basal ganglia: immunohistochemical colocalization of the alpha 1 subunit of the GABA<sub>A</sub> receptor, and the GABAR1 and GABAR2 receptor subunits. *J Comp Neurol* 2004;470(4):339–56.
- [103] Charara A, Pare JF, Levey AI, Smith Y. Synaptic and extrasynaptic GABA-A and GABA-B receptors in the globus pallidus: an electron microscopic immunogold analysis in monkeys. *Neuroscience* 2005;131(4):917–33.
- [104] Chen L, Chan SC, Yung WH. Rotational behavior and electrophysiological effects induced by GABA(B) receptor activation in rat globus pallidus. *Neuroscience* 2002;114(2):417–25.
- [105] Monti MM, Laureys S, Owen AM. The vegetative state. *BMJ* 2010;341(aug02 1):c3765.
- [106] de Biase S, Gigli GL, Lorenzutti S, Bianconi C, Sfreddo P, Rossato G, et al. The importance of polysomnography in the evaluation of prolonged disorders of consciousness: sleep recordings more adequately correlate than stimulus-related evoked potentials with patients' clinical status. *Sleep Med* 2014;15(4):393–400.
- [107] Piarulli A, Bergamasco M, Thibaut A, Cologan V, Gosseries O, Laureys S. EEG ultradian rhythmicity differences in disorders of consciousness during wakefulness. *J Neurol* 2016;263(9):1746–60.
- [108] Cruse D, Thibaut A, Demertzi A, Nantes JC, Bruno MA, Gosseries O, et al. Actigraphy assessments of circadian sleep-wake cycles in the vegetative and minimally conscious states. *BMC Med* 2013;11.

- [109] Lechinger J, Bothe K, Pichler G, Michitsch G, Donis J, Klimesch W, et al. CRS-R score in disorders of consciousness is strongly related to spectral EEG at rest. *J Neurology* 2013;260(9):2348–56.
- [110] Lehembre R, Bruno MA, Vanhaudenhuyse A, Chatelle C, Cologan V, Leclercq Y, et al. Resting-state EEG study of comatose patients: a connectivity and frequency analysis to find differences between vegetative and minimally conscious states. *Funct Neurol* 2012;27(1):41–7.
- [111] Sitt JD, King JR, El Karoui I, Rohaut B, Faugeras F, Gramfort A, et al. Large scale screening of neural signatures of consciousness in patients in a vegetative or minimally conscious state. *Brain* 2014;137(Pt 8):2258–70.
- [112] D'Andola M, Rebollo B, Casali AG, Weinert JF, Pigorini A, Villa R, et al. Bistability, causality, and complexity in cortical networks: an *in vitro* perturbational study. *Cerebr Cortex* 2018;28(7):2233–42.
- [113] Chkhenkeli SA, Sramka M, Lortkipanidze GS, Rakviashvili TN, Bregvadze ES, Magalashvili GE, et al. Electrophysiological effects and clinical results of direct brain stimulation for intractable epilepsy. *Clin Neurol Neurosurg* 2004;106(4):318–29.
- [114] Vataev S, Oganesyan G. Effects of uni-and bilateral destructions of the caudate nucleus head by kainic acid on electroencephalogram in the wakefulness–sleep cycle in wistar rats. *J Evol Biochem Physiol* 2000;36(2):155–60.
- [115] Caplan LR, Schmahmann JD, Kase CS, Feldmann E, Baquis G, Greenberg JP, et al. Caudate infarcts. *Arch Neurol* 1990;47(2):133–43.
- [116] Van Der Werf YD, Sadikot AF, Strafella AP, Paus T. The neural response to transcranial magnetic stimulation of the human motor cortex. II. Thalamocortical contributions. *Exp Brain Res* 2006;175(2):246–55.
- [117] Liepert J, Restemeyer C, Munchau A, Weiller C. Motor cortex excitability after thalamic infarction. *Clin Neurophysiol* 2005;116(7):1621–7.
- [118] Miles TS, Ridding MC, McKay D, Thompson PD. Motor cortex excitability after thalamic infarction. *J Clin Neurosci* 2005;12(4):469–72.
- [119] Lutkenhoff ES, Wright MJ, Shrestha V, Real C, McArthur DL, Buitrago-Blanco M, et al. The thalamic basis of outcome and cognitive impairment in traumatic brain injury. *bioRxiv* 2019:669390.
- [120] Schnakers C, Monti MM. Disorders of consciousness after severe brain injury: therapeutic options. *Curr Opin Neurol* 2017;30(6):573–9.
- [121] Thibaut A, Schiff N, Giacino J, Laureys S, Gosseries O. Therapeutic interventions in patients with prolonged disorders of consciousness. *Lancet Neurol* 2019;18(6):600–14.